

Fabrication of Wound Capacitors using Flexible Alkali-Free Glass

Rudeger H.T. Wilke¹, Amanda Baker¹, Chad Hettler¹, Harlan Brown-Shaklee², Patrick O'Malley¹, Raegan Johnson-Wilke¹, Steve Perini¹, Takashi Murata³, Michael Lanagan¹

¹Materials Research Institute, The Pennsylvania State University,
University Park, PA 16802, USA

²Sandia National Laboratories, Albuquerque, NM 87123, USA

³Nippon Electric Glass, Otsu, Shiga, Japan

Abstract

Applications such as inverters, power management in hybrid electric vehicles, or sensors in down-hole drilling operations often require energy storage and power management at elevated temperatures which is well beyond the scope specifications of many of today's ceramic and polymer capacitors. Alkali-free glasses, which exhibit high energy storage densities (~35 J/cc) present a unique opportunity to couple high temperature stability with high breakdown strength and thus provide an avenue for capacitor applications with stringent temperature and power requirements. Because of the relatively low dielectric constant of glass (5.7), devices are required to be fabricated with large volumes of material in order to achieve the desired capacitance. In this manuscript we demonstrate the feasibility of fabricating wound capacitors using 50 μ m thick glass. Capacitors were fabricated from 2.8 meter long ribbons of thin (50 μ m) glass wound into 125-140 mm diameter spools. The capacitors exhibit a capacitance of 70-75 nF with loss tangents below 1%. The wound capacitors can operate up to 1 kV and show excellent temperature stability to 150 °C. By improving the end terminations, the self-resonance can be shifted to above 1 MHz, indicating these materials may be useful for pulsed power applications with μ s discharge times.

I. Introduction

Next generation capacitors need to be capable of storing large amounts of energy and operate at elevated temperatures. Applications ranging from power management in hybrid electric vehicles to pulsed power in down-hole well drilling operate at temperatures in excess of 150 °C [1-3]. BaTiO₃ based ceramics [4] and polymer capacitors such as polytetrafluoroethylene (PTFE), polyimide (e.g., Kapton), polycarbonate (PC), poly(p-phenylenesulfide) (PPS), and fluorine polyester (FPE) simply cannot perform well in these harsh conditions [5, 6] thus necessitating the search for materials with improved temperature stability. In addition, pulsed power capacitors operating at < 1 μ s time scales often suffer from low recoverable energy densities (< 1 J/cc) [7]. It has previously been demonstrated that using glass as the dielectric material for devices in harsh environments is a promising contender [8, 9]. The breakdown strength of alkali-free glass can exceed 1 GV/m, leading to a stored energy density of 35 J/cc [8]. These numbers are higher than have been reported for glass-ceramic composites, which additions of high permittivity fillers such as BST [10]. Even though the glass ceramic composites show higher permittivity values – microstructural defects at the crystalline ceramic/amorphous glass interface can lead to lower breakdown strengths and hence, only modest improvements in the energy storage

density. These results suggest that simply reducing the dielectric breakdown strength by increasing the activation energy for ion mobility within the glass can play a larger role in enhancing energy density than tuning permittivity.

It should be noted that the alkali-free glasses, along with several other promising high energy density materials [11] are often evaluated in laboratory test conditions – that is, volumetric energy density is reported based on the dielectric breakdown strength and using the dielectric material's volume. In real world applications the materials will necessarily be de-rated and the volume of the packaged capacitor, not just the material, must be taken into consideration. Even so, the impressive numbers for Alkali-free glass may give rise to high voltage capacitors with energy densities greater than 1 J/cc (depending upon Weibull modulus and the packaging scheme). In addition to the excellent room temperature properties of these glasses, the permittivity, loss, energy storage density, and power storage density [12-15] exhibit minimal temperature dependence up to 175 °C[16]. Although the high temperature properties are highly dependent upon the sodium impurity concentration [17].

Aside from the fact that working with glass poses challenges because of its brittle nature, a more significant challenge is related to the fact that it is difficult to extract large capacitance values from the capacitor due to the relatively low dielectric constant. Therefore, creative approaches must be sought out to maximize the amount of stored charge in these materials. Many of the glass manufacturers (Schott, NEG, etc.) have developed processes that allow for fabrication of glass as thin as 5 μm . With the reduction in thickness, the glass becomes sufficiently flexible to envision reel-to-reel manufacturing of wound glass capacitors. Figure 1 plots the bending stress of thinned glass. It can be seen that for a yield stress of 73.6 GPa (the published value for Corning's Willow glass [18]), the minimum achievable bend radius drops below 5 mm for glass thinned below 10 μm . To date, no commercial glass manufacturer sells glass rolls approaching these thicknesses. While it is possible to thin glass via etching in HF and fabricate nF sized capacitors by stacking many layers in an MLCC type geometry, the promise of reel-to-reel processing warrants investigation into the viability using glass in a wound capacitor. In this manuscript we demonstrate for the first time the feasibility of making wound glass capacitors. Specifically, the processing and properties for a 70 nF capacitor produced using 2.8 m of 50 μm thick NEG Ultra-Thin Glass [19].

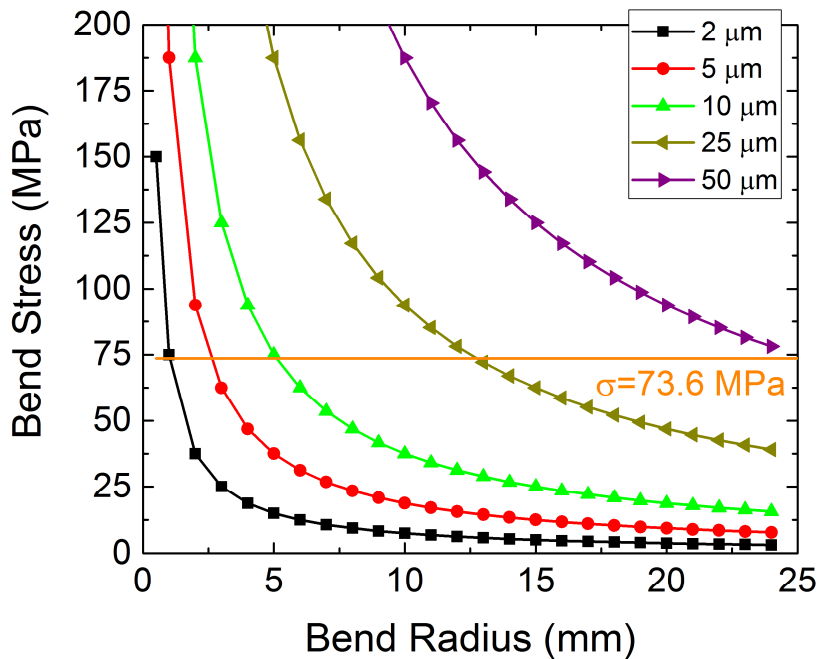


Figure 1 Calculated bending stress as a function of bend radius and glass thickness.

II. Experimental Methods

A. Fabrication of Wound Capacitor

Figure 2 shows a schematic of the unrolled capacitor stack. The 50 μm glass is masked on one side to define a top electrode (blue) and coated on the edges with polypropylene to prevent flash over by providing sufficient edge margin (green). In order to reduce the equivalent series resistance (ESR) and decrease the inductance of the wound capacitor, aluminum termination tabs extend 5 mm beyond the edges of the glass [20, 21].

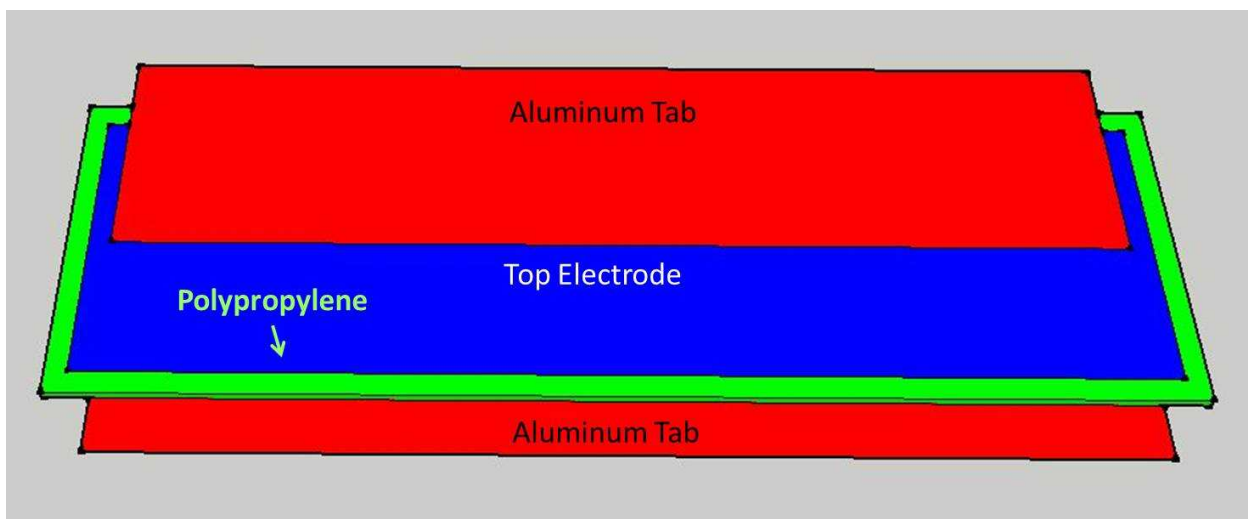
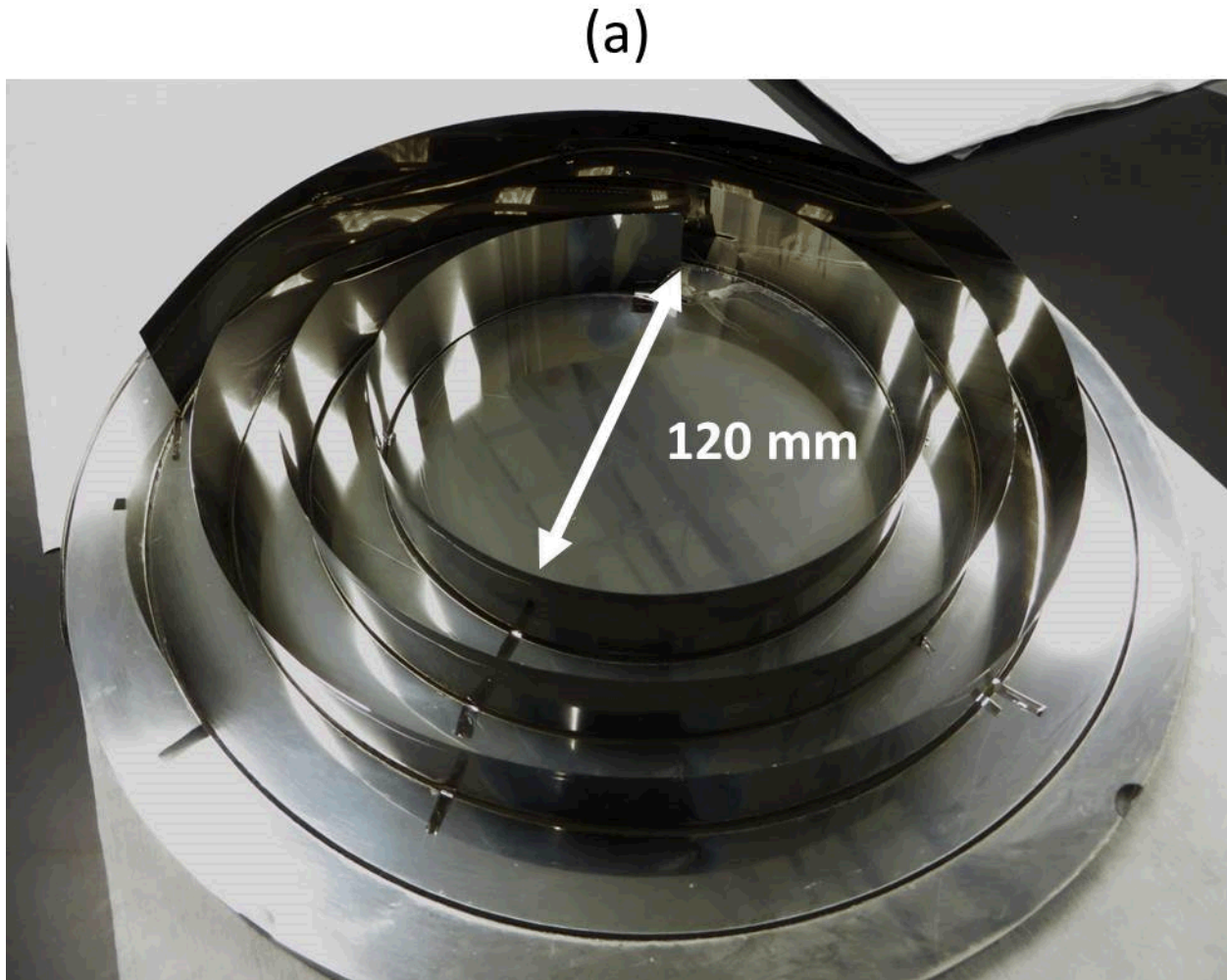


Figure 2 Schematic of the capacitor stack (not to scale). The bottom electrode spans the entire underside of the glass, with the top electrode electrically isolated using polypropylene strips. The aluminum tabs serve to reduce both the equivalent series resistance and inductance of the capacitor, thereby raising the self-resonance frequency.

In order to fabricate the device, the 2.8 m long, 30 mm wide glass was first masked with an acrylic mask to define the top electrode. The entire glass piece was then wound into an Archimedean spiral defined by $r = 60 + \frac{10}{\pi}\theta$ (mm), and loaded into a Semicore Electron Gun Evaporator. The Al contacts were deposited in two steps. First, 4000 Angstroms of Al was deposited on one side of the wound structure. For the second deposition, the glass was unwound from the spiral and rotated 180 degrees about the long axis prior to rewinding in the spiral. This step was necessary to promote thickness uniformity of the Al layer across the width of the film. Shadowing and thickness non-uniformity were a result of finite angle between the sample and the source in the evaporator chamber. A nominal thickness of 4000 angstroms was deposited on each side of the spiral (Figure 3a).



(b)

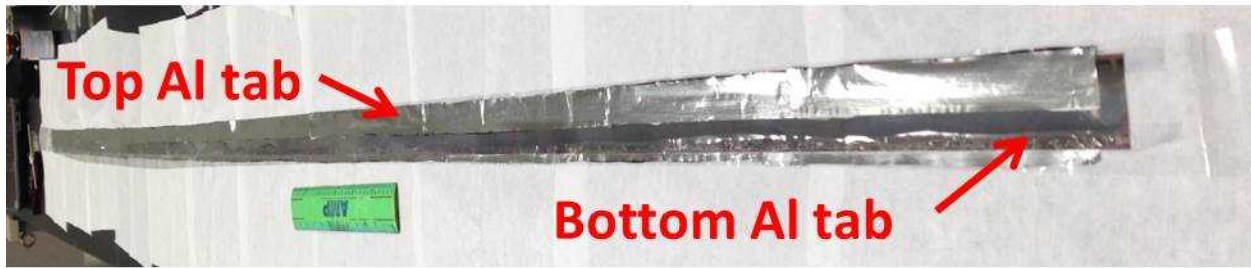


Figure 3 (a) Photograph of the electroded capacitor wound within the Archimedean spiral holder. (b) Unwound glass with Al termination tabs.

After the electrodes were deposited and the sample was unrolled and the mask removed, it was found that the resistance along the 2.8 m Al contact was 40Ω , while the total capacitance was $\sim 70 \text{ nF}$. This corresponds to an RC time constant of $2.8 \mu\text{s}$ ($\sim 360 \text{ kHz}$). With these time constant values, in order to operate the device above 1 MHz, edge termination is necessary to limit the equivalent series resistance (ESR). To provide an effective end termination, two additional processing steps were required. First, 7.5 mm wide x 12 μm thick polypropylene sheets were glued to the edge of the glass to electrically isolate the edges of the sample and prevent shorts between the bottom and top electrodes (Figure 2). Next, 20 mm wide Al sheets, extending 5 mm beyond the edge of the glass were attached using silver paint (Figure 3b).

In order to make the wound capacitor structure, the glass was wound around a 5.5 inch ($\sim 140 \text{ mm}$) polyethylene spool. It should be noted the 70 mm radius of curvature was chosen merely to be conservative on this demonstration sample. The glass is rated to a bend radius just below 40 mm [19]—indicating tighter spirals are possible. Silver paint was applied at four points per turn to promote electrical contact between the Al tabs on successive turns. Figure 4 shows the wound capacitor.

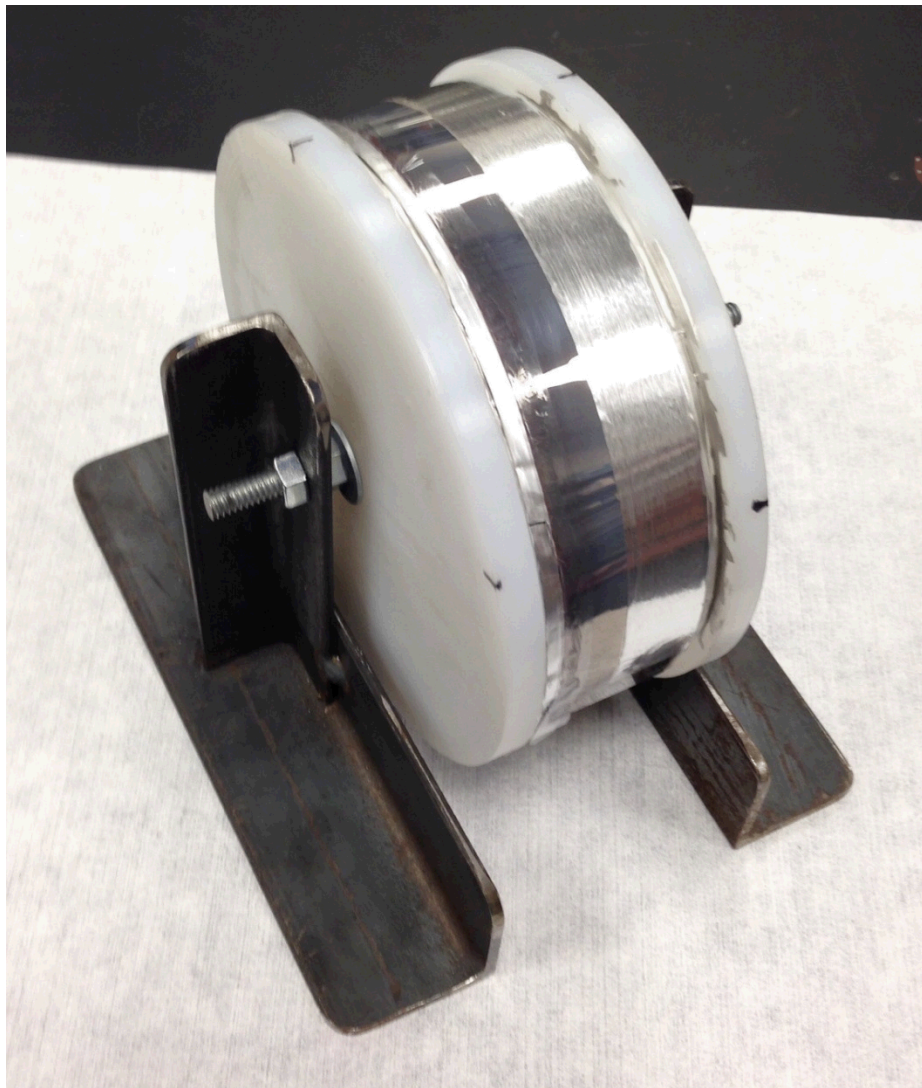


Figure 4 Photograph of the wound capacitor. The 2.8 m glass is wrapped around a 140 mm diameter spool.

B. Electrical Characterization

In order to perform electrical measurements, silver wires were attached to the top and bottom electrodes using silver paint and soldered to contact points on the external case of the capacitor. The capacitance was measured using an HP4294 Impedance Analyzer run by the GADD software (Electrical Characterization Laboratory at Penn State). To reduce the effects of cabling on the sample response, a short compensation was applied. The DC bias dependence of the capacitance was measured at 10 kHz as a function of DC bias up to 1 kV using a custom built biasing tee coupled to a HP4284 LCR meter [22]. The bias tee was calibrated using standard air gap capacitors. The temperature dependence of the capacitance was measured in a Delta Design DD9023 Environmental Test Chamber.

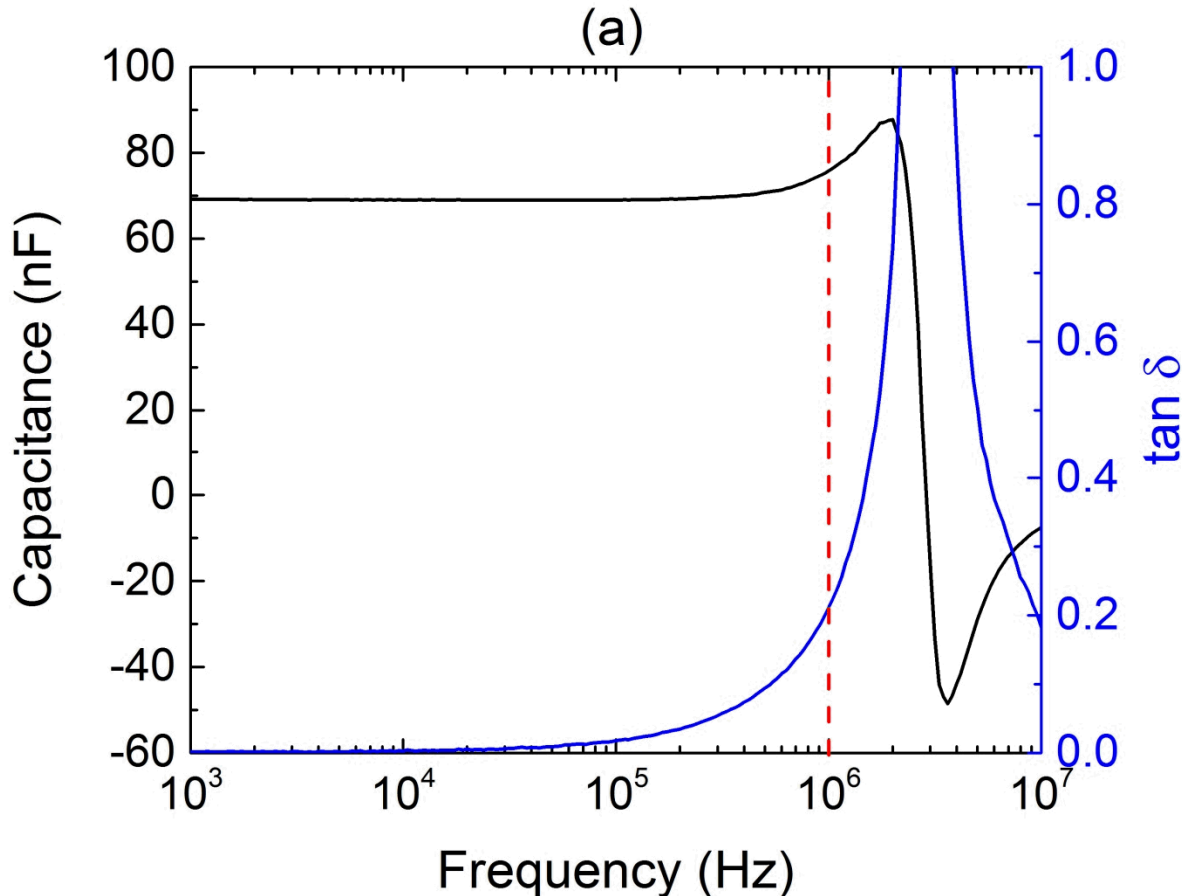
Pulsed discharge measurements were performed by monitoring the current and voltage for an RLC decay. The capacitor was charged to 1 kV using a Keithley 237 source meter and discharged through a 0.245 ohm current viewing resistor (CVR). The voltage across the capacitor and the CVR were recorded using a LeCroy Waverunner 104Xi Oscilloscope. The data were then fit to standard series RLC circuit elements to extract the equivalent series resistance and parasitic inductance of the circuit.

III. Results and Discussion

A. Room Temperature Properties

The low frequency (10 kHz) capacitance of the wound capacitor was 69 nF with a loss tangent of 0.2%. The sample shows roll off at higher frequencies owing to a self-resonance at 3 MHz (determined by the maximum in $\tan \delta$). At 1 MHz the capacitance is 76 nF with $\tan \delta \sim 0.21$ (Figure 4a). Using the relationship

$$\omega = \sqrt{\frac{1}{LC}}, \text{ this implies an equivalent series inductance of } 41 \text{ nH.}$$



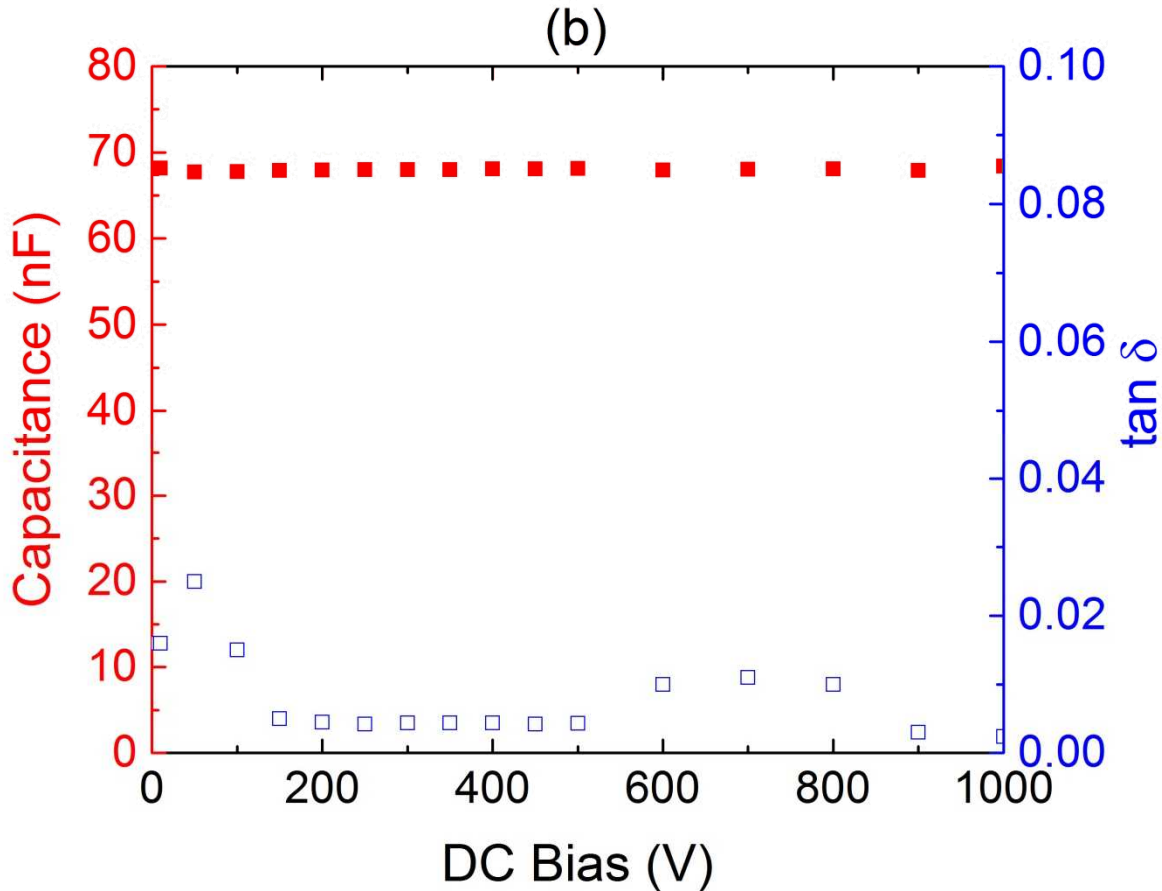


Figure 4 Capacitance and loss measurements of the wound glass capacitor. (a) Frequency dependence of the capacitance and loss at zero bias. (b) Capacitance and loss as a function of DC bias to 1 kV.

Although this loss is too high for practical applications, it demonstrates the feasibility of using wound capacitors for pulsed power applications operating at 1 μ s. The key is simply increasing the resonance frequency by further decreasing the ESR and ESL. There are several approaches that should enable improved frequency response. First, for the ESR value, the width of the capacitor can be decreased so that the impedance across the width of the contacts is decreased. If a true reel to reel process is employed to fabricate future devices, then the potential loss in capacitance from the decrease in area can easily be compensated by an increase in capacitor length. The loss in capacitance can also be compensated by simply using thinner glass. Manufacturers such as NEG, Schott [23], and others have demonstrated the capability of manufacturing glass thinner than 50 μ m, which will allow for increased capacitance, tighter bending radii, and higher energy density capacitors. The bend radius of the glass scales with the inverse of the thickness, indicating that it is possible to reduce the radius of the capacitor to below 15 mm if glass as thin as 10 μ m can manufactured [19]. The second route to decreasing ESR is to terminate the capacitor using a dipping process similar to what is used in MLCCs [24] or wound polypropylene capacitors. This would insure better electrical contact between the termination tabs and the successive turns of the spiral. (It should be noted that this was not performed for this particular

sample as the hand winding of the capacitor did not lead to a high packing density, thus making it difficult to ensure a dipping process did not result in an electrical short between the top and bottom electrodes. With a machine winding process this can readily be avoided.)

Figure 4b shows the DC bias dependence of the capacitance. The capacitor exhibits a flat response with no measurable change in the capacitance up to 1 kV. While this represents a field of only 20 MV/m, it should be noted that thinned Corning Willow glass with a planar geometry ($t= 15 \mu\text{m}$, $C=1.55 \text{ nF}$) exhibits no appreciable tuning of the capacitance out to fields of $\sim 70 \text{ MV/m}$ (data not shown). We have therefore not yet begun to approach the field range where losses within the dielectric begin to play a role. While a myriad of breakdown data exists within the literature, to the authors' knowledge, tests of the dielectric non-linearity of these glasses do not yet exist - perhaps owing to the difficulty in obtaining glass of sufficient thicknesses needed to perform dielectric tunability tests at high electric fields. The data here show that for relatively thick capacitors the dielectric properties of the glass are insensitive to the application of 1 kV.

Pulsed discharge measurements were performed up to 1000 V to test the capacitor for pulsed power applications. The current exceeded 200A with a rise time of $\sim 0.5 \mu\text{s}$. The raw data demonstrate that the series RLC circuit is in an underdamped condition and were fit to a standard series RLC circuit (Figure 5) using the equation:

$$I(t) = \frac{V_0}{\omega L} e^{-Rt/2L} \sin(\omega t)$$

where $\omega = \sqrt{\frac{1}{LC} - \left(\frac{R}{2L}\right)^2}$. The resistance, inductance, and capacitance were set as free parameters and the fit was obtained by using a Levenberg-Marquardt algorithm in LabVIEW. The underdamped state arises from the relatively large inductance from both the circuit and the capacitor. Fits to the data yield an ESR of $\sim 0.43 \Omega$ (after taking the 0.245Ω current viewing resistor into account) and a total inductance of $1.3 \mu\text{H}$. It is believed that the much of this inductance is a result of the measurement circuit. The $>30\times$ increase from the value mentioned above is a consequence of the difficulty to compensate for the inductance of the lead wires necessary to connect to the capacitor (as was done in the case of the C(f) measurement using the HP4294). In order to push these values to higher currents at shorter time scales it is necessary to limit the total inductance of the system. By switching to a MLGC capacitor design as mentioned previously, it is envisioned that the capacitor dimensions can not only be reduced, but it would be possible to mount the capacitor to a low inductance circuit board and achieve more practical current values from an RLC discharge measurement.

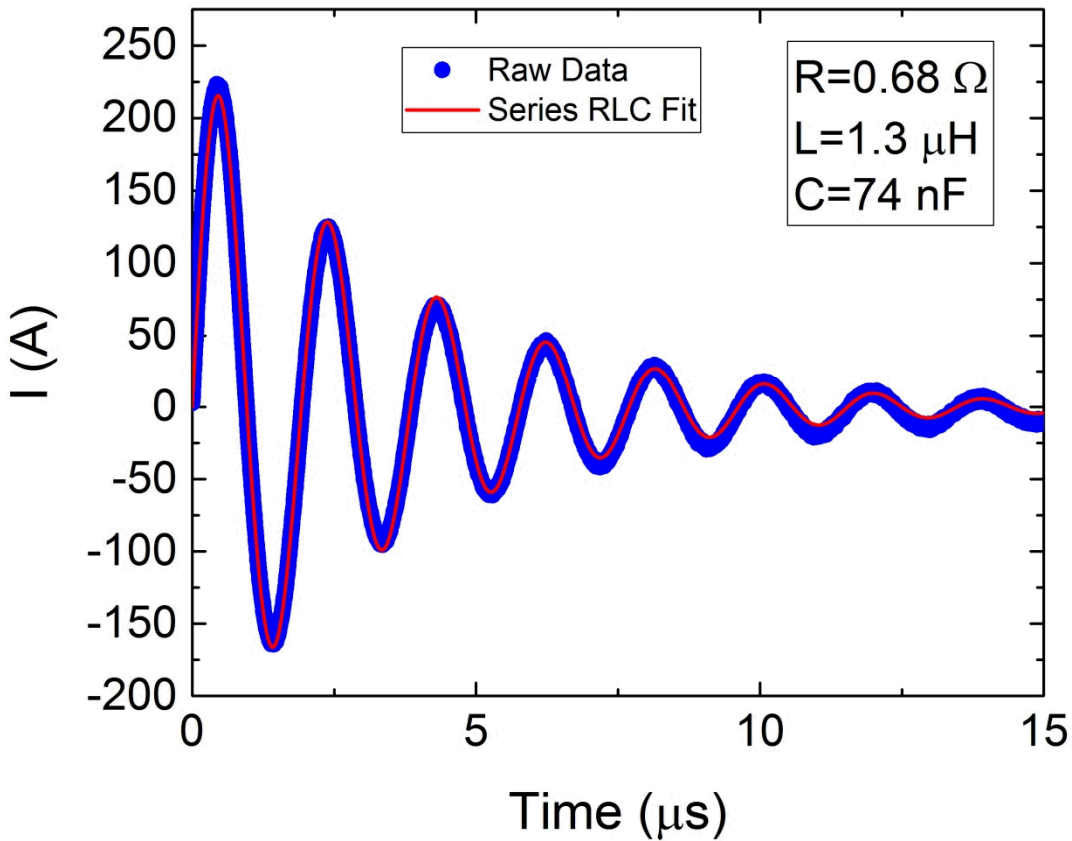


Figure 5 Pulsed-discharge measurement. The capacitor was charged to 1000 V and discharged across a 0.245Ω resistor. The solid line is a fit to an underdamped RLC circuit for extracting the equivalent series resistance and inductance of the discharge circuit.

B. Temperature Dependence of Capacitance

In order to test the temperature dependence of the properties of the wound glass capacitor, a second coil was fabricated. Two significant changes were made. First, air dried silver paste was applied as an electrode. The capacitor was not hermetically sealed and it was therefore necessary to use metal electrodes that were more resistant to oxidation. Second, the capacitor was wound around an alumina core, so that the thermal expansion of the spool would not lead to cracking of the glass capacitor. (The core in this case was 125 mm in diameter.)

It was found that the self-resonance of the capacitor was near 450 kHz, which may reflect a higher ESR from the spray on silver paint electrodes than was observed for the evaporated aluminum.

Consequently, the temperature dependence of the capacitance and loss were only measured up to 100 kHz (Figure 6). Over the frequency range measured, there is little change in the properties of the capacitor. As the temperature is increased, a slight increase in the capacitance and loss are observed. The capacitance increases by an average of 1.5% from 25 °C to 150 °C. At the same time, the loss increases but remains below 1% for all frequencies. The higher loss observed in the 100 kHz measurement is a reflection of its proximity to the aforementioned resonance.

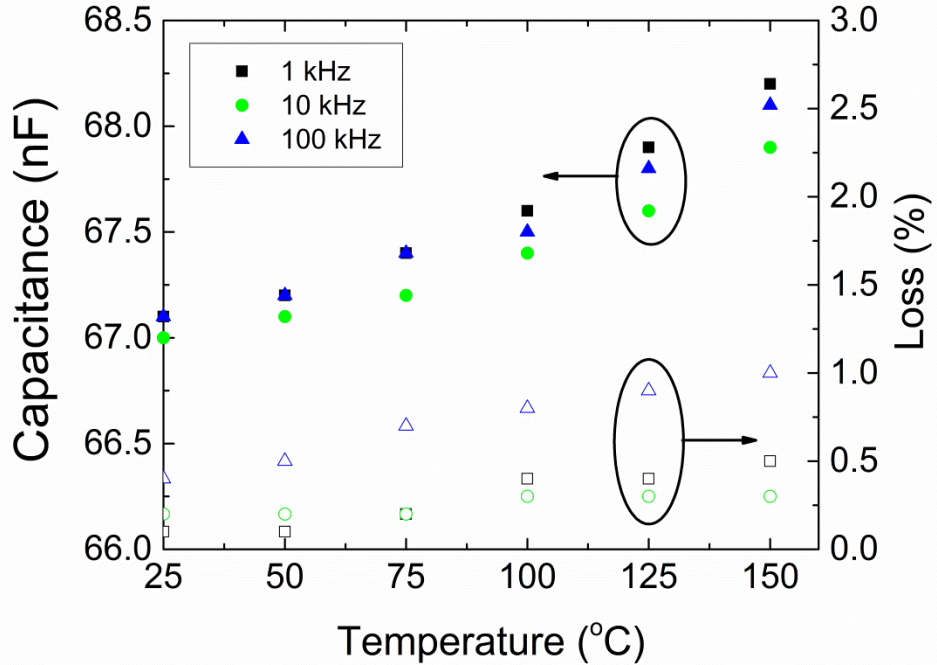


Figure 6 Temperature dependence of capacitance and loss. The change in capacitance over the measured 125 °C range is ~ 1.5%. The loss remains less than 1% even at 150 °C for all measured frequencies.

IV. Conclusion

70 nF capacitors have been fabricated using thin, alkali-free flexible glass. The 2.8 m capacitors were wound into ~70 mm radius spools and tested up to 150 °C. The capacitors showed excellent temperature stability, breakdown strengths above 1 kV. Using Al tabs to terminate the ends of the electrodes, it was possible to push this resonance beyond 1 MHz. Pulsed discharge tests show that while overall circuit inductance is high, the device can push in excess of 200 A in under 1 μ s. In a production environment where reel to reel processing can be employed, it is envisioned that longer length, higher capacitance devices can be produced with lower ESR and ESL values. Conversely, both these values could also be reduced using a multi-layer capacitor strategy. Either should enable the use of glass capacitors for pulsed power applications in extreme temperature environments that can also operate at

sub- μ s time scales. With emerging glass manufacturing technology pushing the limits of glass thickness to 5-10 μ m, it will soon be possible to fabricated wound capacitors under 15 mm in diameter – making them sufficiently small to use in a myriad of applications.

Acknowledgements

We would like to thank Tim Klinger for assistance in the fabrication of the capacitors and Jeff Long for help with the electrical characterization. Sandia National Laboratories is a multi-program laboratory managed and operated by Sandia Corporation, a wholly owned subsidiary of Lockheed Martin Corporation, for the U.S. Department of Energy's National Nuclear Security Administration under contract DE-AC04-94AL85000.

References

1. Johnson, R.W., Evans, J. L., Jacobsen, P., Thompson, J. R. R., Christopher, M., *The changing automotive environment: High-temperature electronics*. IEEE Transactions on Electronics Packaging Manufacturing, 2004. **27**(3): p. 164-176.
2. Buttay, C., Planson, D., Allard, B., Bergogne, D., Bevilacqua, P., Joubert, C., Lazar, M., Martin, C., Morel, H., Tournier, D., Raynaud, C., *State of the art of high temperature power electronics*. Materials Science and Engineering B-Advanced Functional Solid-State Materials, 2011. **176**(4): p. 283-288.
3. Sarjeant, W.J., Zirnheld, J., MacDougall, F. W., *Capacitors*. IEEE Transactions on Plasma Science, 1998. **26**(5): p. 1368-1392.
4. Lines, M.E., Glass, A.M. , *Principles and applications of ferroelectrics and related materials*. International series of monographs on physics. 1977, Oxford, England: Clarenden Press.
5. Zhang, S., et al., *Semicrystalline Polymers with High Dielectric Constant, Melting Temperature, and Charge-Discharge Efficiency*. Ieee Transactions on Dielectrics and Electrical Insulation, 2012. **19**(4): p. 1158-1166.
6. Venkat, N., Dang, T. D., Bai, Z. W., McNier, V. K., DeCerbo, J. N., Tsao, B. H., Stricker, J. T., *High temperature polymer film dielectrics for aerospace power conditioning capacitor applications*. Materials Science and Engineering B-Advanced Functional Solid-State Materials, 2010. **168**(1-3): p. 16-21.
7. MacDougall, F.W., et al., *High energy density pulsed power capacitors*. Ppc-2003: 14th Ieee International Pulsed Power Conference, Vols 1 and 2, Digest of Technical Papers, ed. M. Giesselmann and A. Neuber. 2003. 513-517.
8. Smith, N.J., Rangarajan, Badri, Lanagan, Michael T., Pantano, Carlo G., *Alkali-free glass as a high energy density dielectric material*. Materials Letters, 2009. **63**(15): p. 1245-1248.
9. Demko, R., *Performance Characteristics of Multilayer Glass Dielectric Capacitors*. 2006, AVX Corporation: Raleigh, NC.
10. Gorzkowski, E.P., et al., *Glass-ceramics of barium strontium titanate for high energy density capacitors*. Journal of Electroceramics, 2007. **18**(3-4): p. 269-276.

11. Michael, E.K. and S. Trolier-McKinstry, *Cubic Pyrochlore Bismuth Zinc Niobate Thin Films for High-Temperature Dielectric Energy Storage*. Journal of the American Ceramic Society, 2015. **98**(4): p. 1223-1229.
12. Thienot, E., Domingo, F., Cambril, E., Gosse, C., *Reactive ion etching of glass for biochip applications: Composition effects and surface damages*. Microelectronic Engineering, 2006. **83**(4-9): p. 1155-1158.
13. Kato, Y., Yamazaki, H., Watanabe, T., Saito, K., Ikushima, A. J., *Early stage of phase separation in aluminoborosilicate glass for liquid crystal display substrate*. Journal of the American Ceramic Society, 2005. **88**(2): p. 473-477.
14. Kato, Y., Yamazaki, H., Tomozawa, M., *Detection of phase separation by FTIR in a liquid-crystal-display substrate aluminoborosilicate glass*. Journal of the American Ceramic Society, 2001. **84**(9): p. 2111-2116.
15. Eichler, K., Solow, G., Otschik, P., Schaffrath, W., *BAS (BaO center dot Al₂O₃ center dot SiO₂)-glasses for high temperature applications*. Journal of the European Ceramic Society, 1999. **19**(6-7): p. 1101-1104.
16. Manoharan, M.P., Zou, Chen, Furman, Eugene, Zhang, Nanyan, Kushner, Douglas I., Zhang, Shihai, Murata, Takashi, Lanagan, Michael T., *Flexible Glass for High Temperature Energy Storage Capacitors*. Energy Technology, 2013. **1**(5-6): p. 313-318.
17. Patey, T.J., Schlegel, C., Logaskis, E., *Glass as dielectric for high temperature power capacitors*. MRS Proceedings, 2014. **1679**.
18. Corning. 2015; Available from: <http://www.corning.com/displaytechnologies/en/products/flexible.aspx>.
19. NEG. 2013; Available from: <http://www.neg.co.jp/JP/technology/pdf/idw11.pdf>.
20. Kalina, R.F., *Method of making extended foil capacitors*. 1966: USA.
21. Loescher, D.H., Sidnell, N. A., *Film Capacitors with Low Internal Inductance*. IEEE Transactions on Parts Hybrids and Packaging, 1977. **13**(4): p. 399-402.
22. Moses, P. *High Voltage Blocking Circuits for Permittivity Measurements*. Available from: <http://www.personal.psu.edu/faculty/p/j/pjm112/PDF/BC.PDF>.
23. Schott. http://www.us.schott.com/advanced_optics/english/products/wafers-and-thin-glass/glass-wafer-and-substrates/ultra-thin-glass/index.html. 2013.
24. Moulson, A.J., Herbert, J.M., *Electroceramics : Materials, Properties, Applications*. 2nd ed. 2003, Hoboken, NJ: Wiley.